Final Report on NASA Grant NGR-47-005-081

Applications of Shearing and Kosters Prisms of the Alignment of Optical Telescope

by

Laurence W. Fredrick and Paul H. Knappenberger

LEANDER McCORMICK OBSERVATORY
UNIVERSITY OF VIRGINIA • CHARLOTTESVILLE

July, 1968

Applications of Shearing and Kosters Prisms to the Alignment of Optical Telescopes

Laurence W. Fredrick and Paul H. Knappenberger, Jr.

INTRODUCTION

The purpose of this grant was to examine in detail the application of the wave shearing and Kosters interferometers to detecting misalignment in telescope systems. The small size and light weight of these prism interferometers makes them ideally suited for use in orbiting telescopes and could replace costly lasar techniques for collimation. The results of extensive investigations with the WSI and Kosters prisms at McCormick Observatory have led to the following general conclusions: the Kosters prism is extremely sensitive to non-symmetry of wave form, hence ideally suited for detecting decollimation in optical systems; to evaluate the type and amount of misalignment in the optics with the Kosters prism, requires recognition of a deformed fringe pattern; results of tests have shown that atmospheric turbulence causes the fringe pattern to continually charge shape to the extent that integration over a period of time to eliminate the seeing effects cannot be used successfully. The Kosters prism, therefore, must be limited to testing for decollimation in the laboratory or above the earth's atmosphere.

The WSI, on the other hand, although not as sensitive as the Kosters prism to misalignment, can be used successfully on earth based telescopes, both visually and photographically, to detect decollimation. A catalog of interference patterns for various types and amounts of misalignment in a Cassegrain type reflector has been compiled using three different

shearing interferometers. This report includes the description of the work which led to the aforementioned conclusions and photographs of the interference patterns produced by the prism interferometers under various test conditions. The WSI alignment catalog is included along with an outline of the steps necessary to collimate a two-element reflector.

In addition to the above work, the possibility of using the Kosters prism as a double star or stellar diameter interferometer was investigated. The results are very encouraging.

COLLIMATION OF ASTRONOMICAL TELESCOPES USING THE WSI

A. Introduction

The misalignment of optical elements in astronomical telescopes can be a serious drawback in almost every area of observational astronomy. Aside from the obvious effects of image deterioration in planetary observations, there are serious consequences which are realized in the field of stellar spectroscopy (Petrie 1962). Two areas in which the WSI is particularly suited for application are in telescope collimation techniques for astrometric reflectors and earth-orbit telescopes. The problem of aligning the optical elements of a telescope in orbit about the earth can be solved in a relatively inexpensive way by using the small, compact and light weight shearing interferometer in the manner described below.

In a collimated telescope whose optical elements are figures of revolution, the on-axis wave front will be very symmetrical, and, if free from spherical aberration, nearly spherical in shape barring the effects of mounting cell tensions. For an off-axis image point the wave front will be unsymmetrical, assuming the characteristic comatic shape. The misalignment of optical elements in reflecting or refracting telescopes produces a wave front similar to that characteristic of the third-order coma effect.

The WSI permits an analysis of the wave front to be made and departures from symmetry in the wave front affect the interference fringes in definite ways. For a collimated telescope it is possible to locate the optical axis accurately, by carrying out detailed reduc-

tions of the WSI interferogram data, or approximately, by visual inspection of the fringe pattern. The limit for visually determining the location of the optical axis with the WSI depends upon the observer's ability to detect certain departures of the interference fringes from straightness, parallelism or equal spacing and on the magnitude of the shear angle. (The greater the shear angle, the more sensitive is the technique.) Hence, for a given magnitude of shear, there is a limiting "circle of uncertainty" such that for an interior image point, departures of the fringes from ideal conditions cannot be detected visually, but only by exact measures.

The following discussion will deal with a two-element Cassegrain type reflecting system. There are several ways in which misalignment can be introduced into the optical system. Consider first the secondary mirror. It can be tilted about some pivot point near the center of the mirror or it can be displaced laterally. A combination of the above two effects is also possible. Similarly, the primary mirror can either be tilted, laterally displaced or can suffer some combination of the two effects. There arise three distinct cases for misalignment in such a system. For reference, the "system axis" will be defined to be the axis on which the primary and secondary mirror axes must coincide

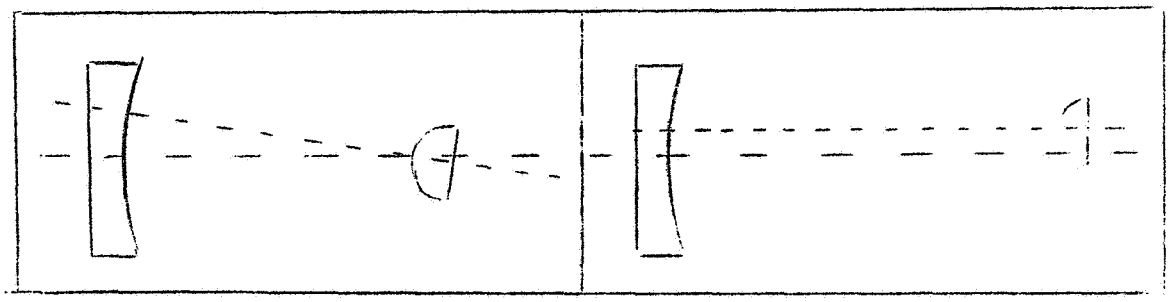

Secondary Tilt Lateral Displacement

for the system to be collimated. An on-axis image will then be an image on the system axis.

Case I: The primary mirror axis is coincident with the system axis but the secondary mirror is misaligned. The on-axis wave front will be unsymmetrical, resembling closely an off-axis wave front in a collimated system. Nowhere will there be a spherical wave front produced. It is then possible to bring the secondary mirror into alignment by examination of the on-axis fringe pattern as will be demonstrated.

Case II: The secondary mirror axis is coincident with the system axis and the primary mirror is misaligned. Once again, an unsymmetrical wave front is produced on the system axis, similar to the off-axis wave front in a collimated system. A spherical wave front is not produced anywhere in the image field for this system. The primary mirror can be brought into alignment by examination of the on-axis fringe pattern as will be described.

Case III: Both the primary and secondary mirrors are misaligned with respect to the system axis. It is possible to compensate for primary mirror misalignment by misaligning the secondary mirror in such a way that a spherical wave front is produced for some image field. This image will lie on the misaligned secondary mirror axis, defining a compensated axis. (See figure 1). Thus, for an image point within the circle of uncertainty surrounding this com-

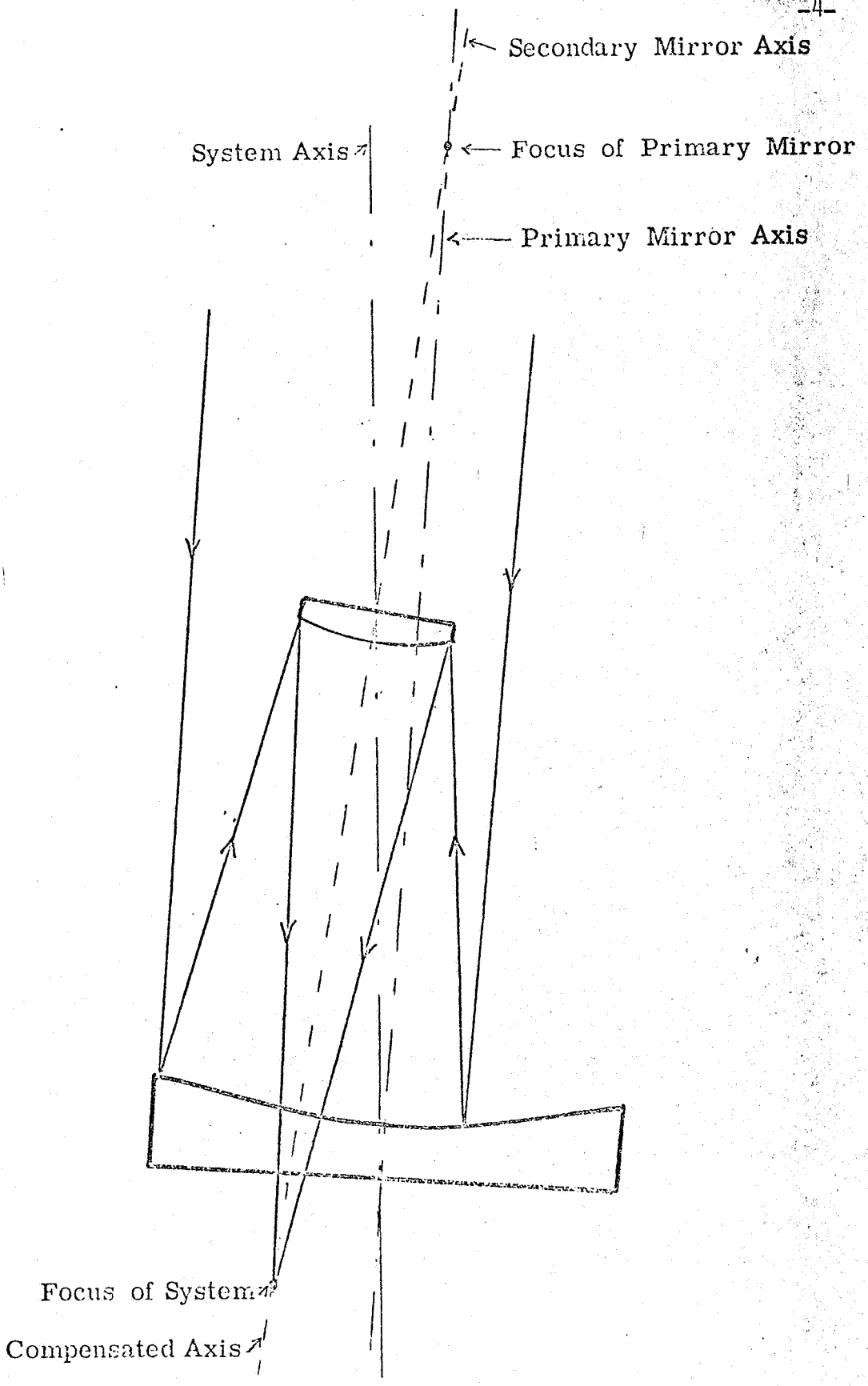

FIGURE 1: Shows primary and secondary mirrors misaligned in such a manner as to produce a spherical wave front on a compensated axis.

pensated axis, the system will produce good fringes. When determining the final collimation in a system where both the primary and secondary mirrors are misaligned, it is necessary to make certain that first, an on-axis image be utilized (i.e. an image on the system axis) and second, that the wave front be analyzed quite precisely.

If either the primary and secondary mirror alignment can be checked independently, cases I and II are relevant, otherwise, the more general case III will be applicable.

B. Equipment

An 8-inch Cassegrain type telescope was used to demonstrate how to collimate a two-element reflector with the WSI. The telescope was modified (see Knappenberger, Wood, and Fredrick 1966) to allow the secondary and primary mirrors to be tilted by a controlled amount. A collimated beam of light produced by a 16-inch parabolic mirror entered the 8-inch optical system and a shearing interferometer mounted in the eyepiece holder produced the interference pattern.

Two different types of shearing interferometers were used to determine what advantages, if any, one type had over the other. Type I had no built-in wedge. Hence, the interference fringes remained always perpendicular to the direction of shear. Type II had a built-in wedge and the fringe rotation was always adjusted so that the fringes were parallel to the shear direction. Two prisms of type II were used, differing greatly in the magnitude of the shear angle. Table 1 lists the properties

of the various WSI prisms.

TABLE 1: WSI PRISMS

prism designation	magnitude of shear	comment
40	0.0026 rad.	no wedge
W	0.0019 rad.	built-in wedge
L	0.0150 rad.	built-in wedge

The following section provides a catalog of interference patterns produced by the above prisms for various telescope misalignments.

C. Alignment Catalog

The effects on the WSI fringe patterns produced by misalignments in a Cassegrain telescope are presented in catalog form. Using this catalog, it is possible to align the optical elements in a Cassegrain system by a visual inspection of the WSI interferograms. The sensitivity of the method depends upon the magnitude of the shear angle, which in practice is limited by the atmospheric seeing conditions.

The direction of shear for all the interferograms presented in this catalog is in the horizontal direction from left to right. This is the fundamental axis from which the direction of tilt of the mirror elements is determined. In plates I, II, and III the secondary mirror is tilted in a direction perpendicular to the shear direction (i.e. about an axis parallel to the shear direction). In plates IV, V, and VI the secondary mirror is tilted in a direction parallel to the direction of shear (i.e. about an axis perpendicular to the shear direction). In plate VII, the

secondary mirror is tilted in a direction 45° to the shear direction. The sign convention for the sense of tilt is as follows.

Plates I, II, III: If the upper edge of the secondary mirror is tilted away from the primary mirror, the tilt is in a positive direction; if tilted towards the primary mirror, the tilt is negative.

Plates IV, V, VI: If the right edge of the secondary mirror is tilted away from the primary mirror, the tilt is in a positive direction; if tilted towards the primary mirror, the tilt is negative.

Plate VII: If the lower right edge of the secondary mirror is tilted away from the primary mirror, the tilt is in a positive direction; if tilted towards the primary mirror, the tilt is negative.

The magnitude of the tilt is expressed in minutes of arc and is the angle formed at the secondary mirror between the optical axes of the primary and secondary mirrors. A description of each plate in the alignment catalog will now be given.

Plate I: Prism 40 was used and the secondary mirror was tilted in a direction perpendicular to the shear direction. The magnitude and sense of tilt are listed under each interferogram. The collimated system is shown by the interferogram labeled 0' and the secondary mirror is tilted in increasing amounts by small steps in the other interferograms. In the upper two rows the fringes are closer together at the top of the pattern and spread outward towards the bottom. The optical axis of the secondary mirror would intersect

the primary mirror above the geometrical center, which corresponds to the direction in which the fringes appear to converge. The lower two rows show fringes which diverge upwards from the bottom of the pattern. For these interferograms, the secondary mirror axis intersects the primary mirror below the geometrical center by increasing amounts as the tilt is increased. For a trained observer, the departure of the fringes from parallelism can be detected by the unaided eye for tilts as small as 9 minutes of arc.

Plate II: Prism W was used and the secondary mirror was tilted in a direction perpendicular to the shear direction. The magnitude and sense of tilt are listed under each interferogram. Once again, the collimated system is labeled 0 and all other interferograms result from a tilted secondary mirror. The sequence of interferograms is identical to that in plate I and the two plates can be compared directly. In the upper rows of plate II the fringes converge towards the right and the secondary mirror axis intersects the primary mirror above the center. In the lower two rows, the fringes converge towards the left and the intersection point is below the center. The shear angle is smaller for prism W than for prism 40, so departures from parallelism are more difficult to detect at 9 minutes of arc in plate II than in plate I.

Plate III: Prism L was used which has the largest shear angle, and again the secondary mirror was tilted perpendicular to the shear direction. The two sheared images of the wave front are more apparent in these interferograms than in plates I and II. The wide vertical black line in all the interferograms is due to the support for the

light source. The fringes behave in the same manner as in plate II except that the effect is more pronounced. An experienced observer can detect misalignment at a tilt angle of only 4.5 minutes of arc using the unaided eye. If the seeing conditions permit use of such a large angle of shear, optical alignment can be done accurately and quickly using the WSI with the unaided eye.

Plate IV: Prism 40 was used, but this time the secondary mirror was tilted in a direction parallel to the shear. As can be noticed in the near-collimated position indicated by zero, there is a residual tilt in the secondary mirror perpendicular to the shear direction. Comparing interferogram zero on this plate with the fringe patterns in plate I, it can be seen that the secondary mirror axis is tilted about -9' to the primary mirror axis. This small residual tilt could not easily be removed using the adjustments available on the secondary mirror, so it remains throughout all the interferograms in plate IV. The effect of tilting the secondary mirror parallel to the shear direction shows up as a curvature and departure from equal spacing in the fringe pattern. In the upper rows the intersection of the secondary mirror axis is to the right of the geometrical center of the primary mirror. Here the fringes are closer together than on the left side. The reverse is true for the interferograms in the lower rows. For prism 40 or any prism of type I, it can be concluded that the fringes are closest together in the direction from the geometrical center of the primary in which the intersection of the secondary mirror axis falls.

Plate V: Prism W was used and the secondary mirror is tilted parallel to the shear direction. Here again, interferogram 0 which represents near-collimation, reveals a residual secondary mirror tilt of -9 minutes of arc perpendicular to the shear direction. Tilting the secondary mirror parallel to the shear direction causes the fringes to curve downward when the intersection point is to the right of center and upward when to the left of center. A less obvious effect is the crowding of the fringes at the top of the fringe pattern when the intersection of the secondary mirror axis is to the right of the primary's center and a crowding at the bottom of the pattern when the intersection is to the left of center.

Plate VI: Prism L was used and the secondary mirror was tilted parallel to the shear direction. Interferogram 0 shows a residual tilt of the secondary mirror of -9' perpendicular to the shear direction. A tilt of only $\pm$4.5' parallel to the shear direction can be noticed in the fringe pattern. By the time the secondary mirror has been tilted 1 , the fringes are already badly deformed. The departures from equal spacing of the curvature in the entire pattern can be noticed easily in this series of interferograms.

Plate VII: This shows the appearance of the interference fringes when the secondary mirror is tilted about an axis 45° to the direction of shear. The fringe pattern in each case is a combination of the patterns obtained when the shear direction is perpendicular or parallel to the secondary tilt. In the method of collimation to be described below, if a pattern such as that in plate VII is obtained, the prism can be rotated until a pattern of pure parallel

tilt or pure perpendicular tilt is achieved. (The dark line pointing towards the upper left is the lever which is used to tilt the secondary mirror and in this case is not coincident with a secondary mirror support).

So far, only the secondary mirror has been tilted while the primary mirror axis remained coincident with the system axis as described in case I of the first section of this paper. What happens when the secondary mirror remains fixed and the primary mirror is tilted? Perhaps not very surprising, the fringes behave in a manner exactly analagous to the case in which the secondary mirror was tilted. If the primary mirror is tilted in a direction perpendicular to the shear direction, and if the top of the primary mirror is tilted away from the secondary mirror, then the interferogram is similar to those in the upper rows of plates I, II, III. The lower rows of plates I, II, III are duplicated when the top of the primary mirror is tilted towards the secondary mirror. Tilting the primary mirror in a direction parallel to the shear with the right edge away from the secondary mirror yields interferograms similar to the upper rows in plates IV, V, and VI and the lower rows in plates IV, V, and VI are similar to the interferograms produced when the right side of the primary is tilted towards the secondary mirror.

There is one distinction, however, not in shape of the fringes but in the amount of distortion. Due to the geometry of the optics in this 8-inch, f/10 Cassegrain telescope with a parabolic 8-inch, f/5 primary mirror and a 3.20-inch hyperbolic secondary located 24.5 inches from the primary mirror, there is almost a 2:1 ratio in the amount of dis-

tortion in the fringe patterns produced by tilting the primary mirror as compared to tilting the secondary mirror. Hence, tilting the primary in a given direction by a given amount produces a fringe pattern exactly like the pattern produced by tilting the secondary mirror in an analogous direction but by an amount almost twice that of the primary tilt. (The exact factor is given by the distance of the primary mirror to the focus divided by the distance of the secondary mirror to the focus, ~1.76.) This effect is shown in plate VIII.

Plate VIII: Prism 40 was used to demonstrate the fringe patterns produced when the primary mirror is tilted. The upper photograph shows the fringe pattern when the primary mirror is tilted perpendicular to the shear direction with the top part of the primary tilted away from the secondary mirror. Even though the tilt angle is only 22 minutes of arc the pattern is analogous to that produced in plate I when the secondary mirror is tilted between 36 and 45 minutes of arc. The middle row shows the effects on the fringes when the primary mirror is tilted in a direction parallel to the shear, the left two interferograms correspond to the right edge of the primary tilted away from the secondary mirror and the right two interferograms correspond to a tilt towards the secondary mirror. These interferograms may be compared to those in plate IV. The lower row shows first, a tilt perpendicular to the shear when the top of the primary is tilted towards the secondary mirror and secondly, an arbitrary tilt of the primary mirror.

With these series of interferograms it now becomes possible to decribe a method for collimating a Cassegrain telescope.

D. Collimation Technique

For a Cassegrain telescope to be correctly aligned, the optical axes of the primary and secondary mirrors must be coincident. When this condition is realized, a WSI interferogram obtained with an on-axis image will show the optical quality of the mirrors. If the telescope is misaligned, the fringe pattern can be made to resemble one presented in this catalog by proper orientation of the shear direction. The technique of collimating a Cassegrain telescope using the WSI will be described for each of the three possible cases of misalignment, assuming that misalignment is due only to tilt and not lateral displacement of the optical elements. The discussion will refer to the particular telescope used in producing the alignment catalog.

Case I: Primary mirror aligned, secondary mirror misaligned.
If the primary mirror can be checked independently and the secondary mirror axis is to be brought into coincidence with the optical axis of the primary mirror, the following procedure is used. The WSI is mounted in the focal plane on the optical axis of the primary mirror (in most cases this will be at the geometrical center of the primary mirror). A star can be used as a light source and the star's image should fall on the optical axis of the primary mirror. This can be accomplished by centering the star's image in an eyepiece reticle. The interference pattern should now be observed and, by rotating the shearing prism about the optical axis of the primary mirror, there will be four positions (corresponding to four directions of shear) in which the observed fringe pattern will

resemble those given in the appropriate plates in the catalog. More specifically, if prism 40 is used, there will be two settings of the prism separated by 180° in which the observed interferogram will resemble one given in plate I of the catalog. At 90° from these two settings there will be two additional prism orientations which show interferograms similar to those given in plate IV. When the above orientations of the prism have been determined, the amount and direction of secondary mirror tilt can be deduced by comparing the observed fringes with those given in the catalog. The proper mirror adjustment should produce straight, evenly spaced, parallel fringes in all directions of shear (this of course depends on the mirror optics), and collimation has been achieved.

Case II: Primary mirror misaligned, secondary mirror aligned. If the alignment of the secondary mirror can be determined independently and the primary mirror is to be tilted to bring its optical axis into coincidence with the secondary mirror axis, then the following procedure is used. The WSI is mounted in the focal plane on the axis of the secondary mirror and the star's image is adjusted so as to fall on this axis. By rotating the shearing prism about the optical axis of the secondary mirror, four directions of shear will be found which produce interferograms similar to those given in the catalog. When the four settings have been determined, the direction of primary tilt can be deduced by interchanging the words "primary" and "secondary" in the description of sign convention for the sense of tilt given in section C, and the magnitude of tilt will be 1.76

times the number listed under the interferogram which matches the observed fringe pattern. The proper mirror adjustment will then assure collimation.

Case III: Primary mirror misaligned, secondary mirror misaligned. Experience has shown that a distorted fringe pattern produced by primary mirror misalignment can be returned to a pattern indicating a spherical wave front by misaligning the secondary mirror to compensate for the asymmetry in the wave front produced at the primary mirror. Thus, acceptable interferograms can be produced when the two mirror axes are not coincident, but merely in a compensated configuration. In such a configuration of the optics, the secondary mirror is laterally displaced from the axis of the primary mirror and also tilted in such a manner as to produce a nearly spherical wave front for some image point in the focal plane. (See figure 1.) No attempt has been made to use the WSI to detect lateral displacement of the optics in a multi-element system.

When collimating a telescope in which both primary and secondary mirrors are misaligned, some technique must be used to bring the mirrors into near alignment such as the eyeball method. An image produced by a spherical wave front at the geometrical center of the primary mirror can be achieved by adjusting the secondary mirror until the fringe pattern is perfect in all directions of shear. This technique will assure an excellent on-axis image but does not guarantee that the off-axis aberrations are as small as

possible. In general, then, to insure a collimated system, both the elements must be adjusted so that not only the on-axis image is acceptable, but also the off-axis aberrations are minimized. It is highly desireable to have an independent method for assuring the alignment of either the secondary or primary mirrors and then resorting to techniques described in cases I or II of this chapter.

E. Conclusions

The collimation technique described above has been tested on the 8-inch Cassegrain telescope in the optics laboratory at McCormick Observatory and is found to be very effective. Viewing the fringe pattern with the unaided eye permits alignment between secondary and primary mirror axes of better than 9 minutes of arc using prism 40, about 12 minutes of arc using prism W and better than 4 minutes of arc with prism L. Thus, the larger the magnitude of shear, the greater the sensitivity of the method. Atmospheric seeing conditions will limit the amount of shear that can be used on any given night. To further reduce the limit for collimation, an eyepiece reticle made up of evenly spaced, parallel lines could be used to view the fringe pattern. Then, subtle departures from parallelism or even spacing in the fringe pattern could be detected. A reticle with a cross hair was tried in the laboratory and by carefully aligning the cross hairs, the limit of collimation was reduced by a factor of 2 or more. Finally, the fringe pattern can be photographed and an enlarged print can be measured to an accuracy of better than 30 seconds of arc in this particular telescopic system.

To extend this technique to other telescopes it is not necessary to compile a new catalog, but rather only scale the amount of tilt to

apply to the different system. The actual distance from secondary mirror to focus and primary mirror to focus for each particular telescope as well as the f/ratios of the system should be taken into account when determining a factor to change the scale of mirror tilt. This factor can be determined by experiment on any particular telescope and the technique described above can then be applied. The question of lateral displacement of the mirrors in a telescopic system has not been dealt with in this paper, but presents a problem for future study.

THE KOSTERS PRISM

A. Introduction

The modified Kosters interferometer, which has been described by Saunders (1957a, 1957b), can prove to be a useful tool in several areas of astronomy. Saunders has suggested use of the Kosters interferometer for testing the optical quality of large telescopes, measuring double star separations and position angles and also for measuring stellar diameters. The Kosters prism seemed to be the ideal solution for detecting misalignment in telescope systems because of its unique properties, so studies were undertaken at McCormick Observatory to verify this statement, as well as to examine the possible use of the prism for stellar diameter measurements. The results of these investigations are presented in this paper.

The Kosters prism interferometer, as described by Saunders, is small, lightweight and quite rigid. When mounted in the eyepiece holder of an astronomical telescope which is directed towards a star, the Kosters prism folds one-half of the converging wave front over onto the other half, provided that the beam dividing plane is adjusted to bisect the optics. A set of interference fringes is produced and, if the star is not resolved, the shape of fringes will be characteristic of the telescope optics. If there is asymmetry in the wave front, the fringes will be distorted. Thus, since a misaligned telescope produces a non-symmetrical wave front, and since the Kosters prism is extremely sensitive to non-symmetrical wave form, the prism should provide an ideal test for decollimation.

B. Equipment

A Kosters prism was obtained by McCormick Observatory and used in the optics laboratory to test for decollimation effects in optical systems. Originally, the 8-inch Cassegrain telescope was to be used in the manner described for producing the WSI alignment catalog. However, it was not possible to obtain a small enough point source or to remove one sufficiently far away in the limited space of the optics laboratory, so that the interference fringes would fill the image field of the 8-inch optics. To obtain a satisfactory set of interference fringes, it was necessary to go to smaller apertures and three different lenses were used throughout the laboratory work. A simple plano-convex lens of 50mm diameter, an aerostigmat f/5, 305mm focal length lens and a 3-inch astronomical refracting telescope were used in tests for decollimation effects and stellar diameter determinations.

The optical arrangement shown in figure 2 was used for the testing. The light source was a special thin filament lamp which simulated a point

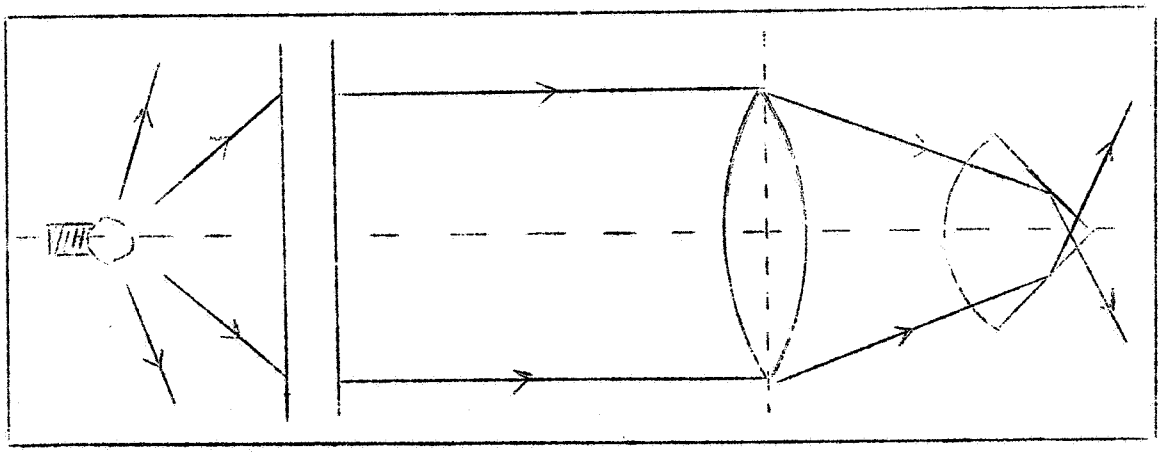

Figure 2 Arrangement of the optical components for laboratory tests using the Kosters prism.

source in one-dimension. The distance from the light source to the lens was about 17 feet for the decollimation tests. The objective lens and Kosters prism were mounted on an optical bench which provided the necessary degrees of freedom for proper adjustment of the optics.

C. Test for Misalignment

Since the 8-inch Cassegrain telescope could not be used with the laboratory light source, some way of simulating misalignment in an optical system had to be found. As was pointed out in the section on collimation of telescopes with a WSI, a misaligned telescope produces a wave front similar to the comatic wave front for an off-axis image produced in an aligned system. It was decided, then, to record the fringe pattern produced by various lenses using off-axis images. Although it is not possible to form a misalignment catalog in this manner, the behavior of the fringe pattern could be noted and the feasibility of using the Kosters prism for collimation work could be ascertained. The fringe patterns resulting from off-axis images in the above mentioned lenses have inherent in them the effects of coma and astigmatism.

While preparing to photograph interferograms produced by off-axis images, an important characteristic of the Kosters prism was noticed. When the light source, lens and prism were properly aligned, the interferograms labeled 0 in plate IX were observed. If the light source was moved a very small angular amount perpendicular to the dividing plane of the prism, the fringes rotated. Moving the light source through an angle of <30 seconds of arc measured from the lens, to the right of its aligned position caused the fringes to rotate as shown in the first interferogram in the top row for each lens in plate IX. Moving the

light source through 9 seconds of arc and then 40 seconds of arc to the left of the aligned position produced the last wo interferograms in the upper rows for each lens in plate IX. This point is mentioned because it forms the basis for using the Kosters prism for stellar diameter measurements, which will be discussed later. Also, when using the Kosters prism on a telescope with a star as the light source, the atmospheric turbidity causes the stars image to dance about, hence the fringe pattern is constantly swinging from side to side, although the fringes are tied down at the dividing plane. The motion of the fringe pattern is a good test of seeing conditions.

To obtain photographs of interferograms for off-axis images, the light source, lens and prism were aligned so the fringe patterns labeled 0 in plate IX were obtained. Now, the lens was rotated through a given angle and the prism was adjusted to bring the fringe pattern into view. To produce the first interferogram in the second row for each lens in plate IX, the lens was rotated by the angular amount shown under the interferogram about an axis perpendicular to the plane of figure 2 and passing through the center of the lens. Thus, the image of the light source was off-axis in a direction perpendicular to the dividing plane of the prism. The distortion of the fringe pattern is immediately obvious and could be detected when the lens was rotated through a much smaller angle than that used to photograph the pattern. Rotating the lens about the same axis but in the opposite direction, produced the second interferogram in the lower row for each lens in plate IX.

The first two interferograms of the lower row for each lens in

plate IX are similar to the interferograms that would be produced if a Cassegrain telescope were misaligned such that either the secondary or primary mirror was tilted in a direction perpendicular to the dividing plane of the prism. The last two interferograms in the same rows as above, are similar to the interferograms which would be produced by a misaligned Cassegrain telescope in which the primary or secondary mirror was tilted in a direction parallel to the dividing plane. These last two interferograms were produced by rotating the lens about the axis shown passing through the lens in figure 2, first in one direction and then in the opposite direction by an amount given under each interferogram. The experiment proved conclusively that the Kosters prism can be used effectively to detect non-symmetries in a converging wave front.

The Kosters prism seemed more sensitive to these asymmetries than the shearing prism and with the use of a very small point source the Kosters prism could be used for alignment of telescopes in a laboratory. To use the Kosters prism on a telescope with a star as the light source was the next step. The prism was mounted at the eyepiece of the McCormick 26-inch refractor. Even though the seeing was good, the fringes waved around and it was not possible to photograph the interference pattern. The fringes could be seen quite easily but because of their motion it would have been difficult to recognize the various patterns which reveal misalignment. It was concluded, therefore, that in the absence of atmospheric turbulence, such as in a laboratory or above the earth's atmosphere, the Kosters prism could be used successfully to detect misalignment, but due to the motions of the fringe pattern when viewing

a light source through the atmosphere, it would be very difficult to recognize a fringe pattern well enough to make the necessary corrections for collimating a telescope.

D. The Kosters Prism as a Stellar Interferometer

Measurements of the angular diameters of stars has always been a fundamental problem in astronomy. Michelson and Pease tried with some success to measure stellar diameters with an optical interferometer. Several problems beset their work, including the adverse effects of seeing on the fringe visibility. The Kosters prism provides a method of measuring stellar diameters by optical interferometry which is not affected by seeing conditions to the extent of the Michelson technique.

When the Kosters prism is mounted at the focus of an astronomical telescope and a point source is located on the extension of the dividing plane of the prism, a set of interference fringes is seen, such as shown in the interferogram labeled 0 for the aerostigmat in plate IX. If another point source were located to the right of the dividing plane, such as would be the case for a double star properly oriented, another set of interference fringes would be produced, similar to the interferogram labeled -15" for the aerostigmat in plate IX. Now, the two sets of fringes would be superimposed and would interfere with each other, alternately re-enforcing and destroying the contrast between dark and light fringes. As a result, a series of dark and bright bands (nulls) will appear across the interferogram parallel to the dividing plane. The separation between adjacent dark or bright bands is inversely proportional to the separation of the point sources. This relationship is expressed as

follows

$$d'' = \frac{\lambda}{4S} \times 206265''$$

where d is the angular separation between the point sources

λ is the wavelength being used

S is the distance from the dividing plane to the first fadeout.

Consider an extended source. It can be treated as if it were made up of many individual point sources at different distances from the extended dividing plane of the Kosters prism. Each of these individual point sources produces its own set of interference fringes which in turn are all superimposed to form the observed pattern. The result is a set of fringes which loses contrast as the distance from the dividing plane increases. The distance from the dividing plane to the place where the fringe contrast has disappeared is inversely proportional to the angular diameter of the extended source. In practice, the fringe contrast as a function of distance from the dividing plane could be measured electronically and a visibility curve for the extended source could be produced. The limiting angular diameter which can be measured with a telescope with aperture A is given by

$$d'' = \frac{\lambda}{2A} \times 206265''$$

The above theory was tested in practice by using a 3-inch astronomical telescope of focal length 37.5 inches and a small thin filament source a large distance away. The upper row of interferograms in plate X was photographed as follows. The center fringe pattern was produced

when the source, lens and prism were as nearly aligned as possible. The left and right interferograms were obtained by shifting the dividing plane of the prism a very small amount to the left and the right. This has the same effect as moving the source off the dividing plane, thus causing the fringes to rotate. As can be seen in the photographs, the fringe visibility as a function of the distance from the dividing plane does not change even when the fringes are rotated. Thus, when using this interferometer to measure a star's diameter, the atmospheric seeing will cause the fringes to rotate, or wave from side to side, but the visibility or contrast in the pattern will not be affected. Rows two and three of plate X were photographed in the same manner as row one but the source was adjusted only slightly to present a more extended area perpendicular to the dividing plane. As the angular size of the source increased, the distance from the dividing plane to the fringe fade out decreased.

E. Conclusions

The possibility of using the Kosters prism as a stellar interferometer was explored. The results are very encouraging. Part of one night was spent on the McCormick 26-inch refractor with the Kosters prism. The fringes produced by a single star were observed and good contrast was seen across the entire fringe pattern. More work involving the Kosters prism is anticipated. The measurement of double star separations and the diameters of the satellites of Jupiter could be measured using the McCormick telescope. Some shop work on an eyepiece mounting which permits the Kosters prism to be oriented correctly in the telescope needs to be completed. This work could demonstrate the feasibility of using the

Kosters prism as a means for determining the angular diameter of stars.

The Kosters prism has shown to be extremely sensitive to asymmetries in a converging wave front and ideally suited for collimating telescopes where there is no atmospheric turbidity. The WSI, however, is better suited for collimation work through the earth's atmosphere because it is not as sensitive to seeing conditions as is the Kosters prism.

REFERENCES

Knappenberger, P. H., Wood, H. J. and Fredrick, L. W. 1966, "Design and Applications of Optical Interferometers in Astronomy," Final Report to NASA on Grant NGR-47-005-031.

Petrie, R. M. 1962, Stars and Stellar Systems, W. A. Hiltner, Ed. (The University of Chicago Press, Chicago), Vol. III, pp. 64-81.

Saunders, J. B. 1957a, J. Res. N.B.S., 58, 21.

_____. 1957b, ibid, 27.

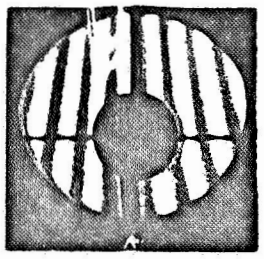

72′

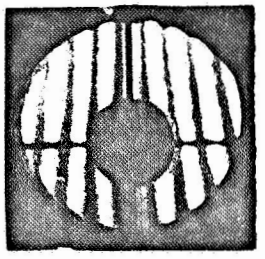

63′

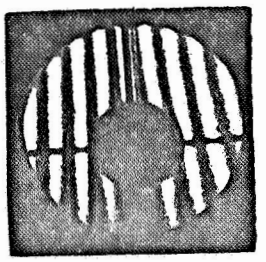

54′

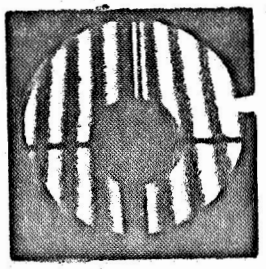

45′

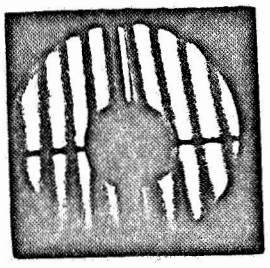

36′

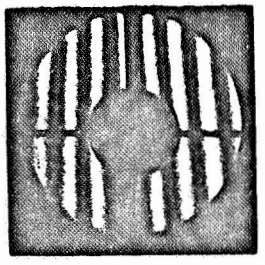

27′

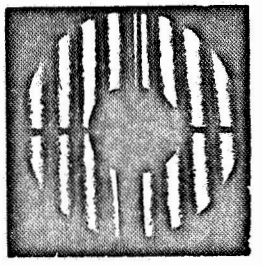

18′

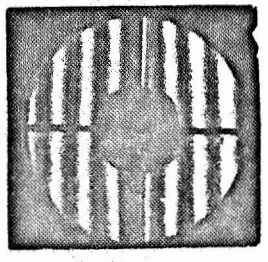

9′

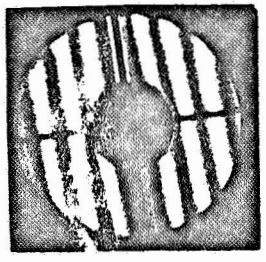

.′5

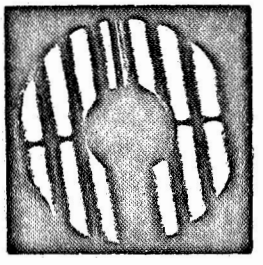

0′

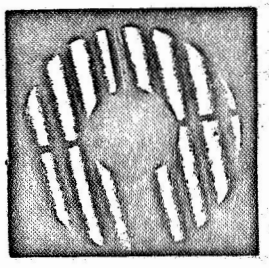

-4.5

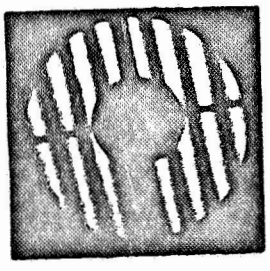

-9′

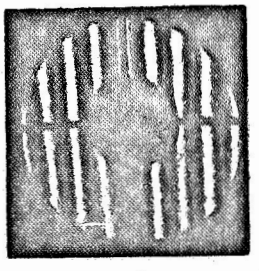

-18′

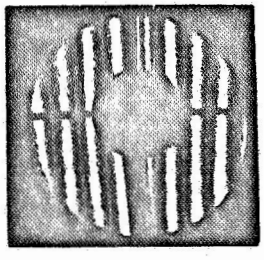

-27′

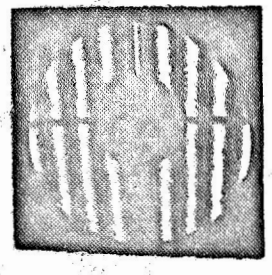

-36′

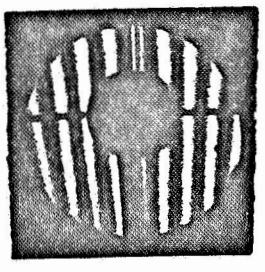

-45′

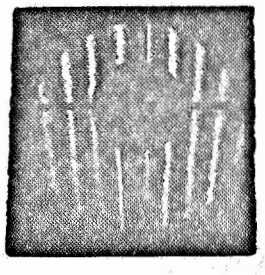

-54′

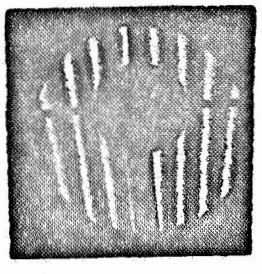

-63′

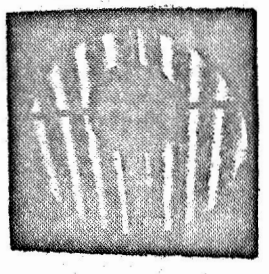

-72′

PLATE I APPEARANCE OF WSI FRINGES WHEN SECONDARY MIRROR IS TILTED BY THE AMOUNT SHOWN UNDER EACH INTERFEROGRAM. PRISM +0 (0 0039 rad.) TILT DIRECTION PERPENDICULAR TO SHEAR DIRECTION

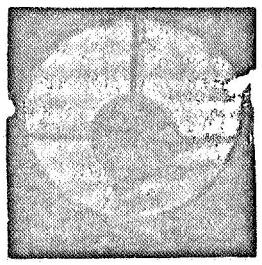

6 3′

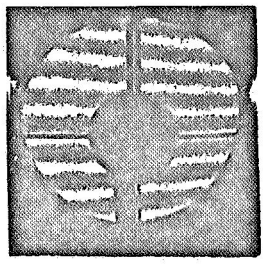

5 4′

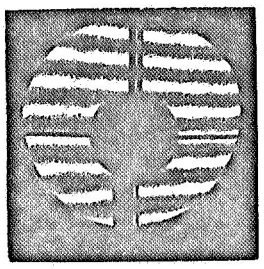

4 5′

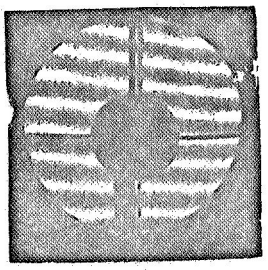

3 6′

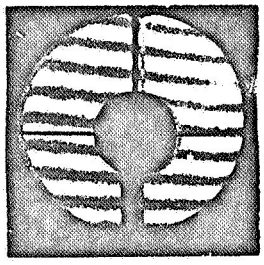

2 7′

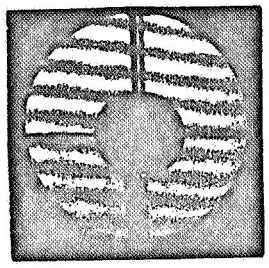

1 8′

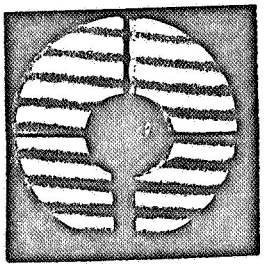

9′

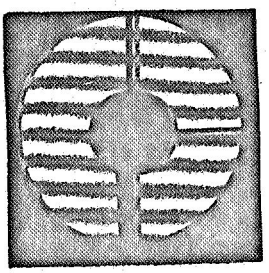

4.5

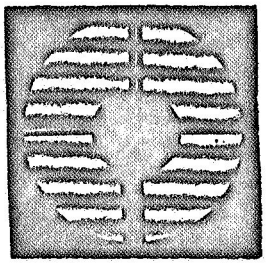

0

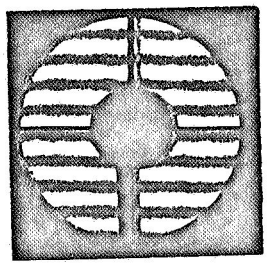

-4.5

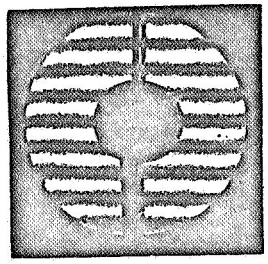

-9′

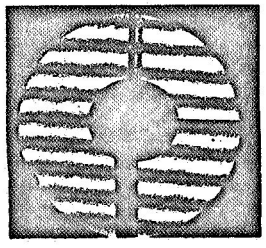

-18′

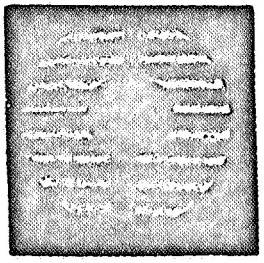

-27′

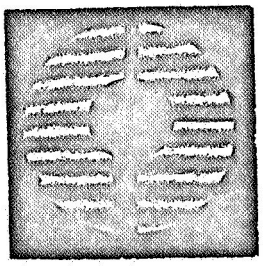

-36′

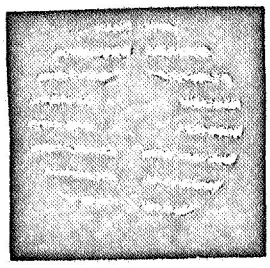

-45′

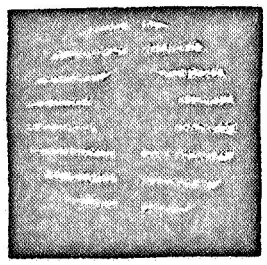

-54′

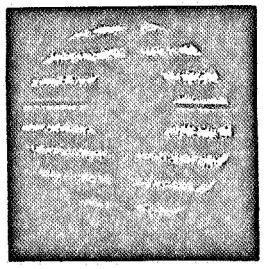

-63′

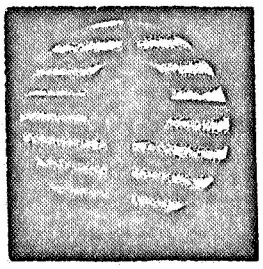

-72′

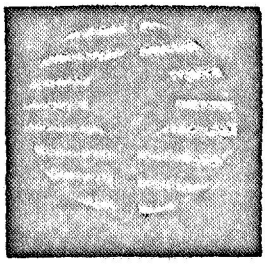

PLATE II APPEARANCE OF WSI FRINGES WHEN SECONDARY MIRROR IS TILTED BY THE AMOUNT SHOWN UNDER EACH INTERFEROGRAM. PRISM W-30 USED (CW) TILT DIRECTION PERPENDICULAR TO SHEAR DIRECTION

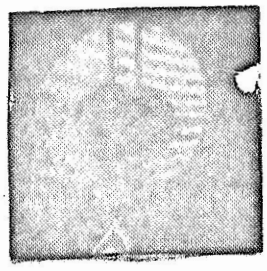

54′

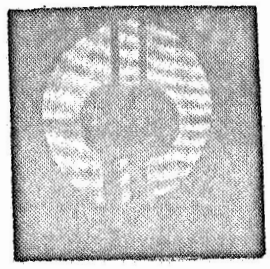

36′

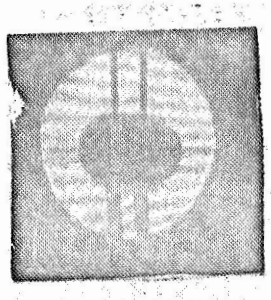

27′

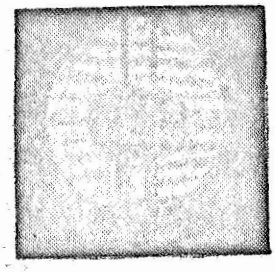

18′

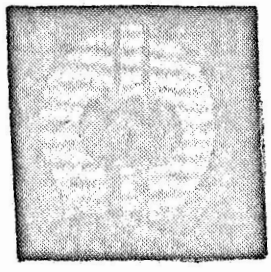

13.5

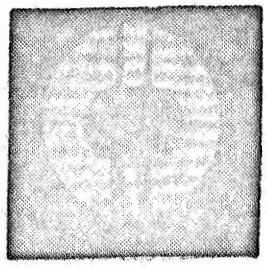

9′

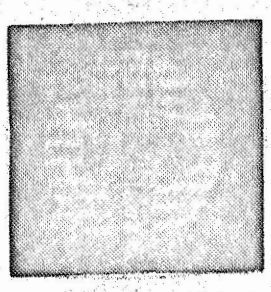

4.5

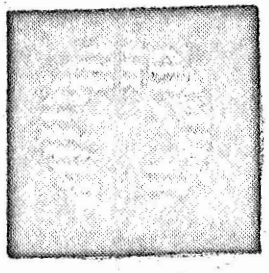

0

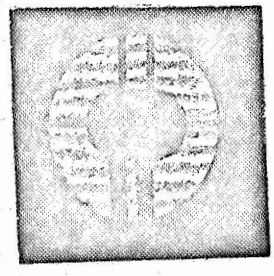

-4.5

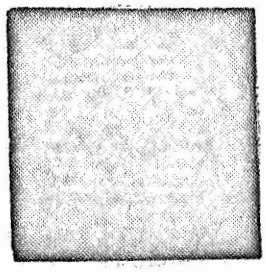

-9′

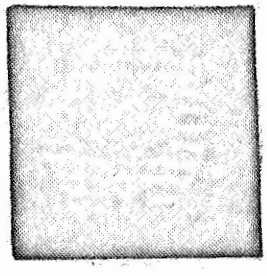

-13.5

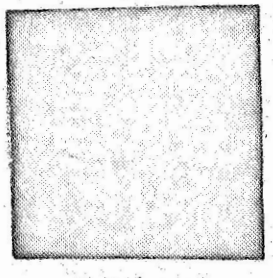

-18′

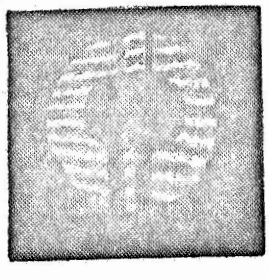

-27′

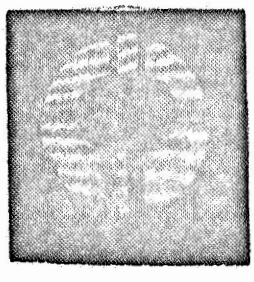

-36′

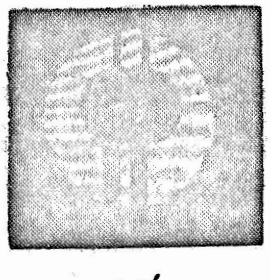

-45′

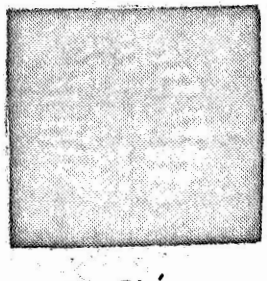

-54′

PLATE III APPEARANCE OF WSI FRINGES WHEN SECONDARY MIRROR IS TILTED BY THE AMOUNT SHOWN UNDER EACH INTERFEROGRAM. PRISM L (0.0150 rad.) TILT DIRECTION PERPENDICULAR TO SHEAR DIRECTION

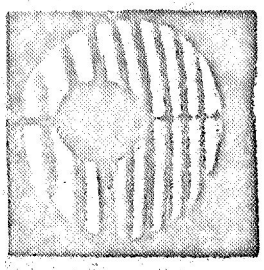

72′

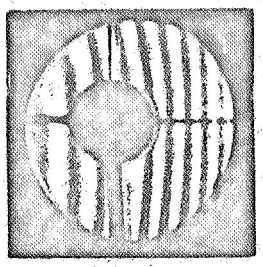

63′

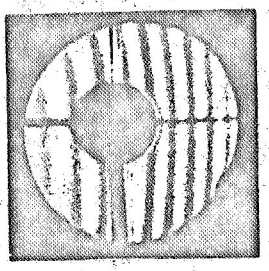

54′

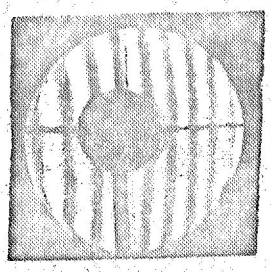

45′

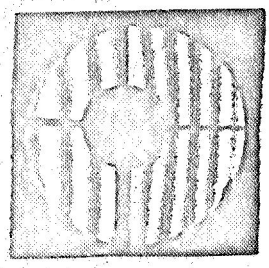

36′

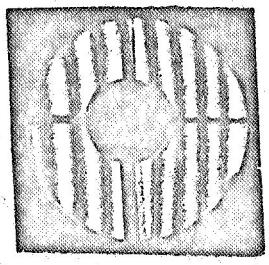

27′

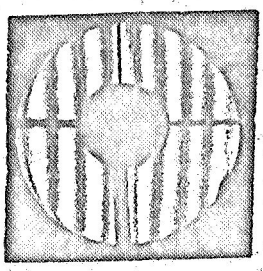

18′

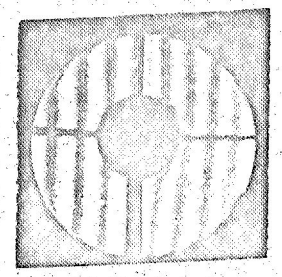

13.5

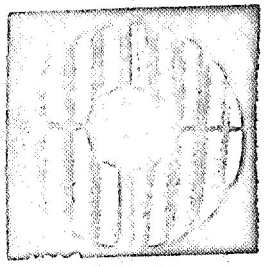

9′

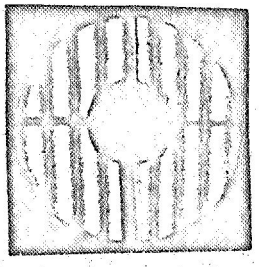

4.5

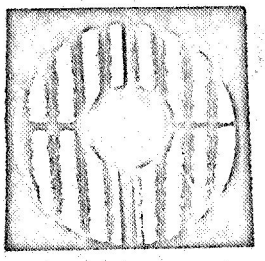

0

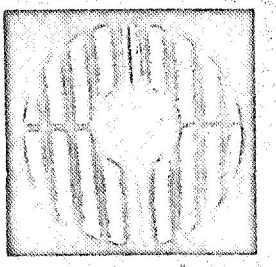

-4.5

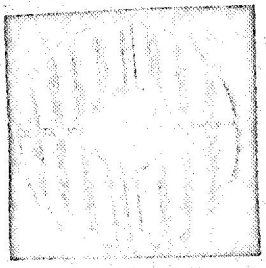

-9′

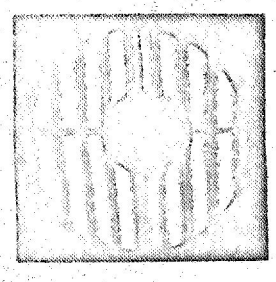

-13.5

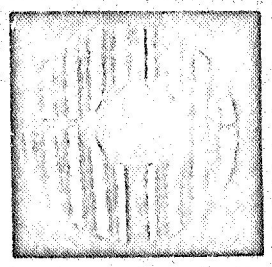

-18′

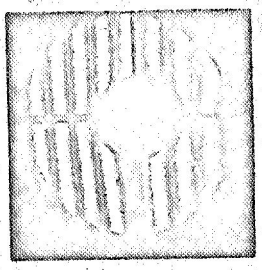

-27′

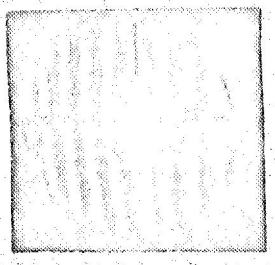

-36′

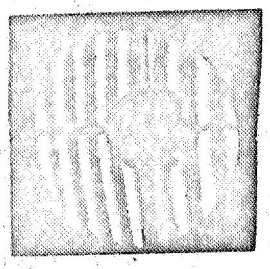

-45′

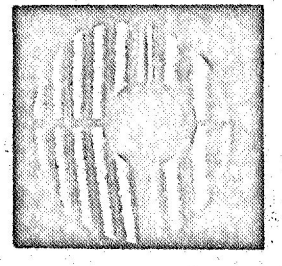

-54′

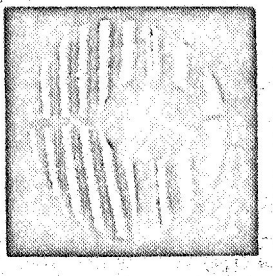

-63′

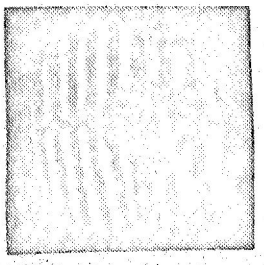

-72′

PLATE IV APPEARANCE OF WSI FRINGES WHEN SECONDARY MIRROR IS TILTED BY THE AMOUNT SHOWN UNDER EACH INTERFEROGRAM. PRISM 40 (0.0039 rad.) TILT DIRECTION PARALLEL TO SHEAR DIRECTION

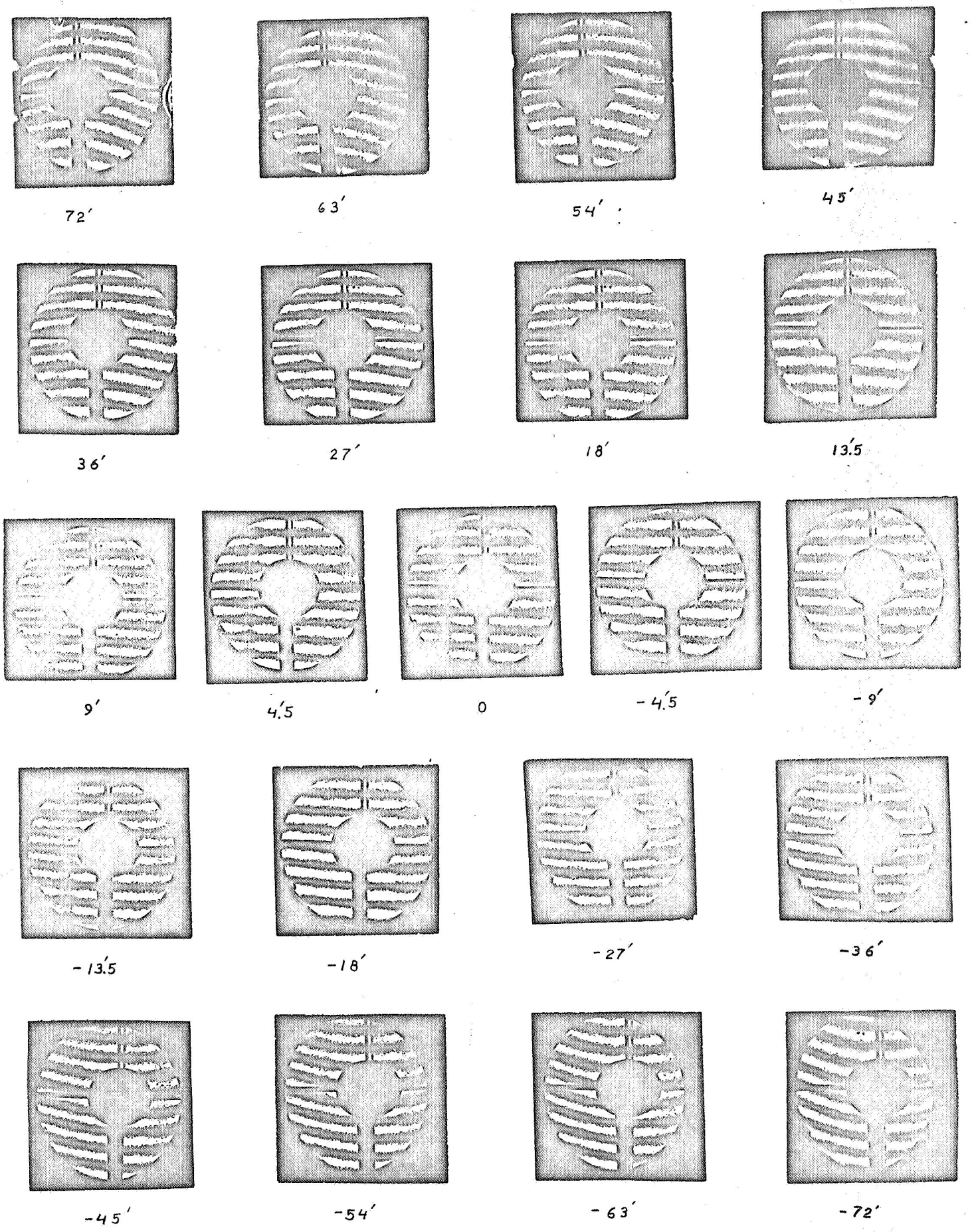

PLATE V APPEARANCE OF WSI FRINGES WHEN SECONDARY MIRROR IS TILTED BY THE AMOUNT SHOWN UNDER EACH INTERFEROGRAM. PRISM W (0.0019 rad.) TILT DIRECTION PARALLEL TO SHEAR DIRECTION

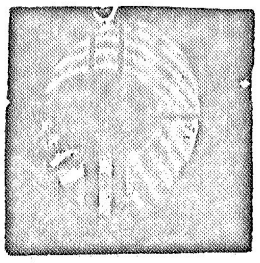

72′

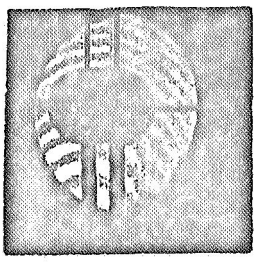

63′

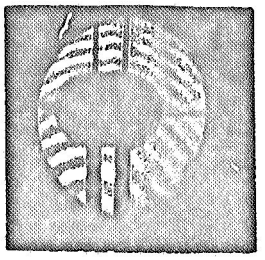

54′

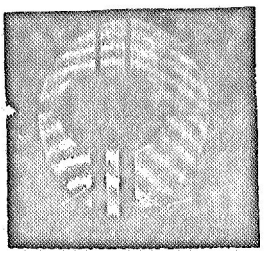

45′

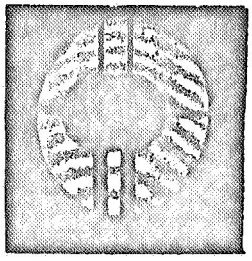

36′

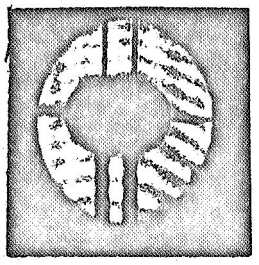

27′

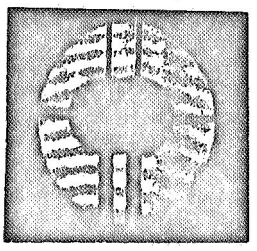

18′

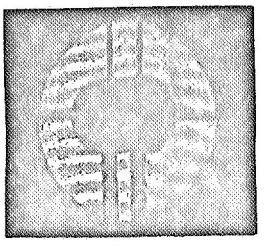

13.5

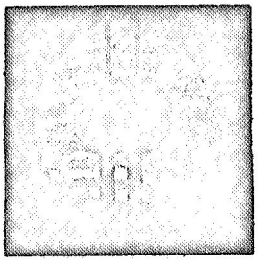

9′

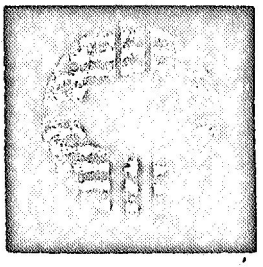

4.5

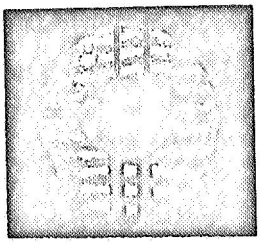

0

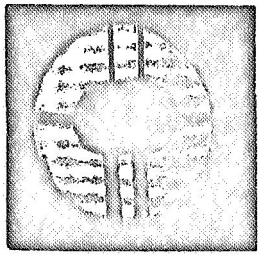

- 4.5

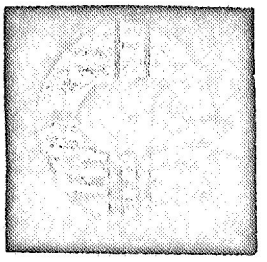

- 9′

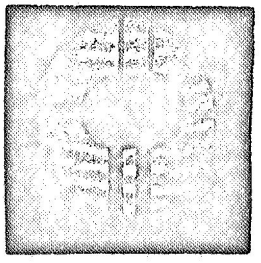

- 13.5

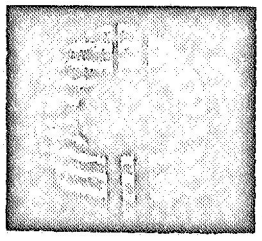

- 18′

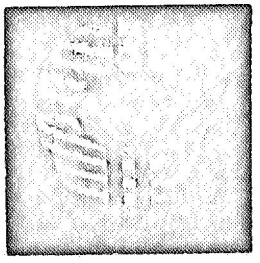

- 27′

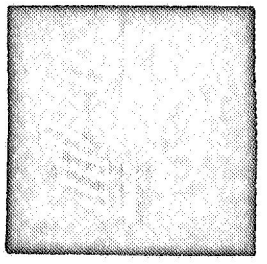

- 36′

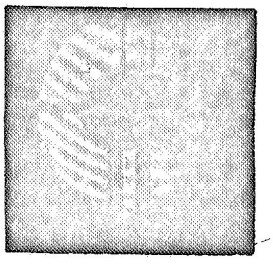

- 45′

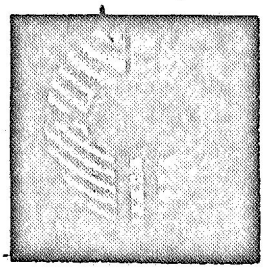

- 54′

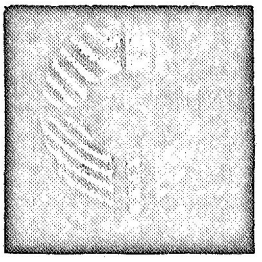

- 63′

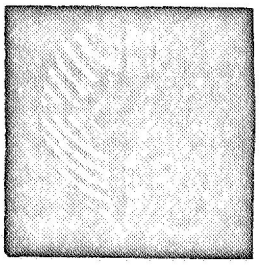

- 72′

PLATE VI APPEARANCE OF THE WSI FRINGES WHEN SECONDARY MIRROR IS TILTED BY THE AMOUNT SHOWN UNDER EACH INTERFEROGRAM PRISM L (0.0156 rad) TILT DIRECTION PARALLEL TO SHEAR DIRECTION

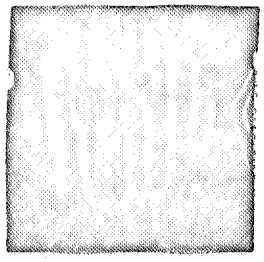

PRISM 46

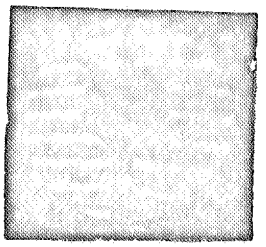

PRISM W

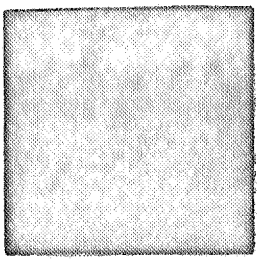

PRISM L

AMOUNT OF TILT +36'

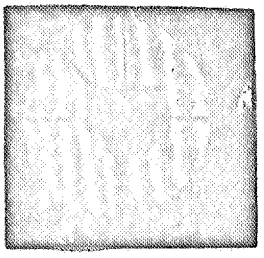

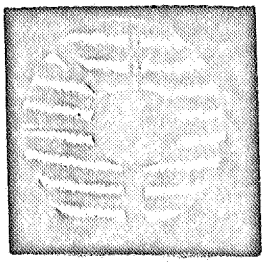

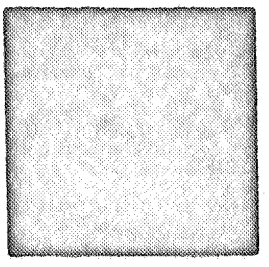

AMOUNT OF TILT -36'

PLATE VII APPEARANCE OF THE WSI FRINGES WHEN THE SECONDARY MIRROR IS TILTED IN A DIRECTION 45° TO THE DIRECTION OF SHEAR.

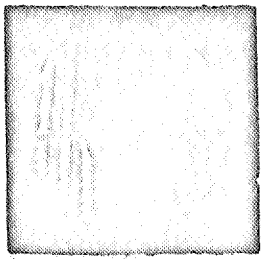

⊥ 22'

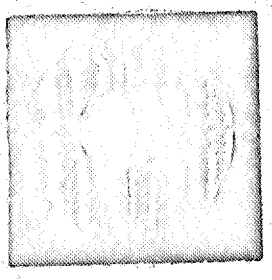

II 16'

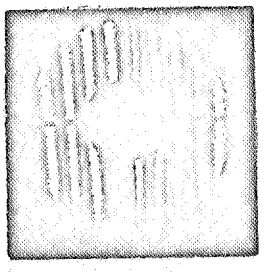

II 5'

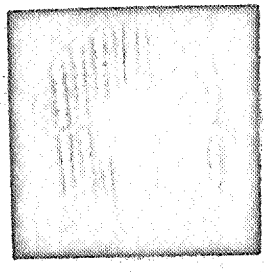

0

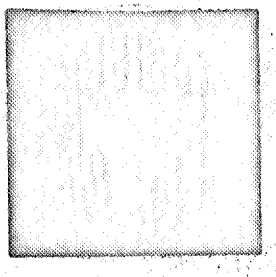

II -5'

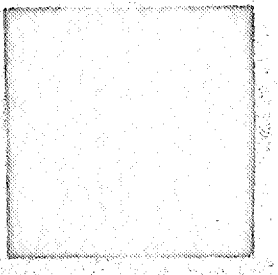

II -16'

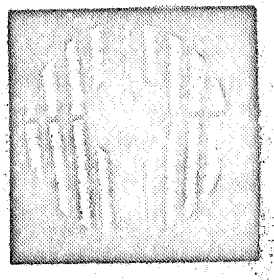

⊥ -22'

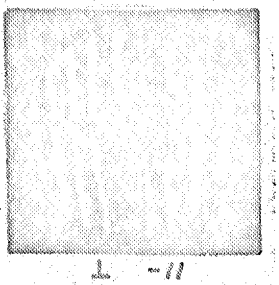

⊥ -11
II -16

PLATE VIII APPEARANCE OF THE WSI FRINGES PRODUCED BY PRISM 46 WHEN THE PRIMARY MIRROR IS TILTED IN THE DIRECTION (RELATIVE TO SHEAR DIRECTION) AND BY THE AMOUNT SHOWN UNDER EACH INTERFEROGRAM.

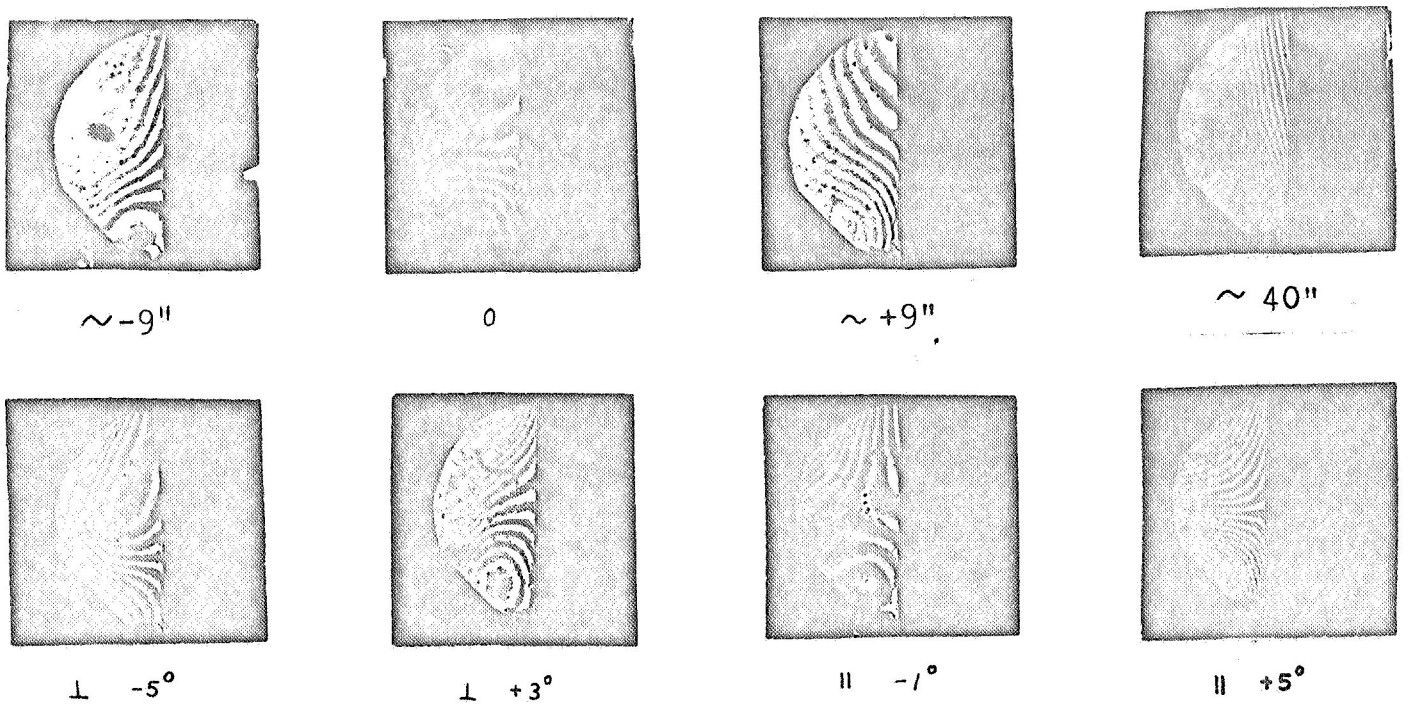

SINGLE ELEMENT PLANO CONVEX F. L. = 308 m.m.

AEROSTIGMAT f/5.0 F. L. = 305 m.m.

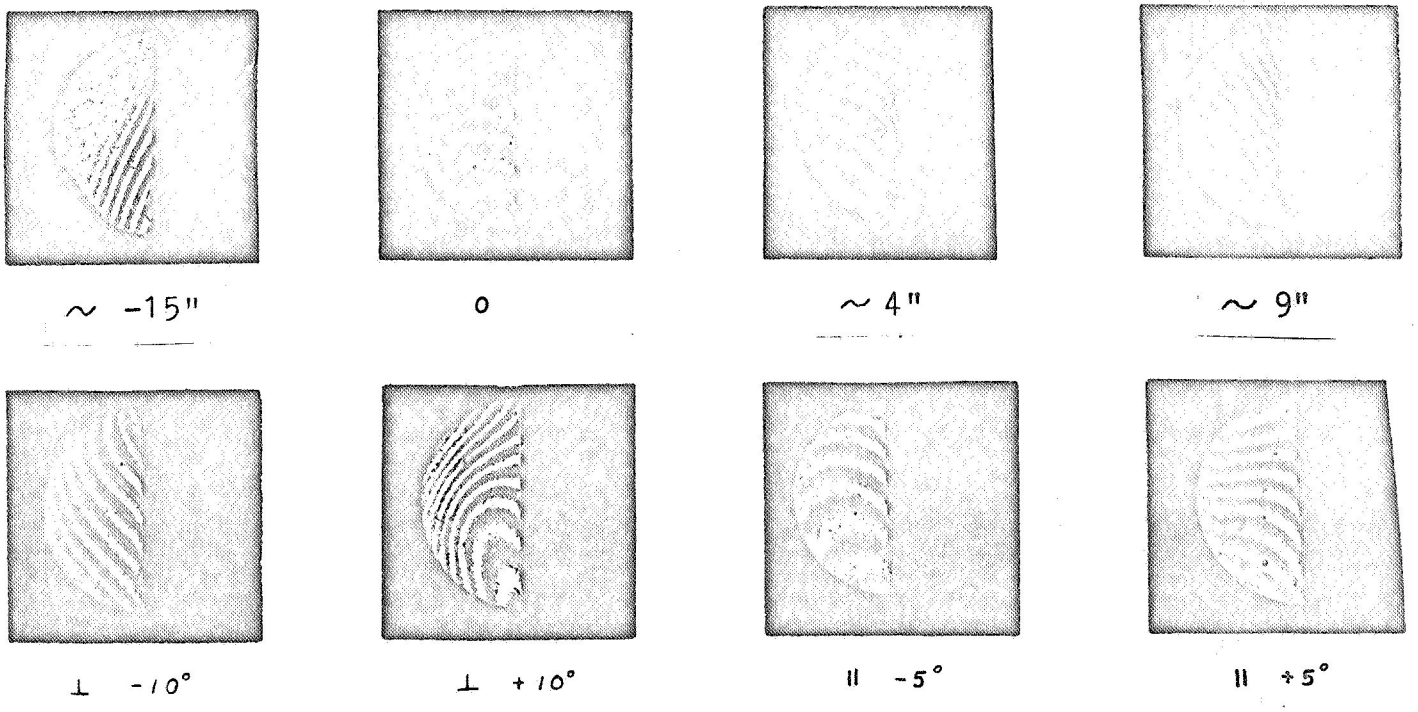

PLATE IV

THE APPEARANCE OF FRINGES PRODUCED BY KOSTER'S PRISM USING A LABORATORY SOURCE AND TWO DIFFERENT LENSES. THE UPPER ROW IN EACH SET WAS PRODUCED BY MOVING THE SOURCE OFF THE OPTICAL AXIS PERPENDICULAR TO THE DIVIDING PLANE BY THE ANGULAR AMOUNT SHOWN. THE LOWER ROW SHOWS THE EFFECTS OF LENS ABERRATIONS; THE IMAGE WAS OFF AXIS IN A DIRECTION RELATIVE TO THE DIVIDING PLANE BY THE ANGULAR AMOUNT SHOWN UNDER EACH INTERFEROGRAM.

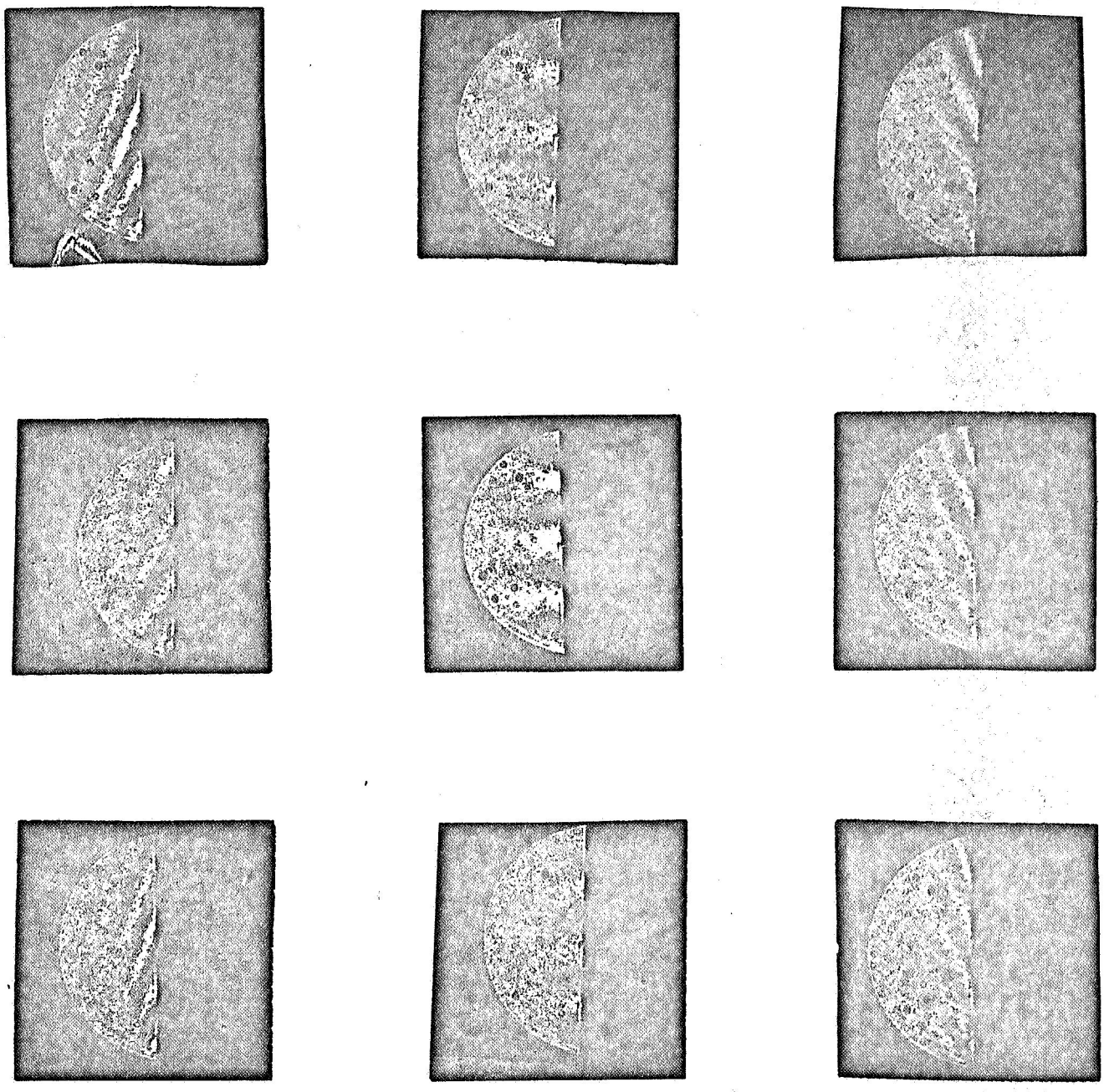

PLATE X THE APPEARANCE OF KOSTER'S FRINGES FOR VARIOUS SOURCE SIZES. THE ANGULAR SIZE OF THE SOURCE INCREASES FROM ROW 1 TO ROW 3, AS DOES THE AREA OF GOOD FRINGE CONTRAST. THE SOURCE IS SLIGHTLY TO THE LEFT OF THE DIVIDING PLANE IN COLUMN 1, ON THE DIVIDING PLANE IN COLUMN 2 AND TO THE RIGHT OF THE DIVIDING PLANE IN COLUMN 3.